



Experimental Study on Horizontal Flame Spread of Dual-Flame Sources for Building Façade Energy Conservation FPU Foam Under the Effect of Lateral Wind

Wei Zhang¹ and Jingwei Wang^{2*}

¹School of Architecture and Planning, Anhui Jianzhu University, Hefei, China, ²Country Garden Company, Hefei, China

OPEN ACCESS

Edited by:

Qiangling Duan,
University of Science and Technology
of China, China

Reviewed by:

Yang Zhou,
Central South University, China
Fei Tang,
University of Science and Technology
of China, China

*Correspondence:

Jingwei Wang
wanlulu2730@163.com

Specialty section:

This article was submitted to
Sustainable Energy Systems and
Policies,
a section of the journal
Frontiers in Energy Research

Received: 01 March 2022

Accepted: 19 April 2022

Published: 31 May 2022

Citation:

Zhang W and Wang J (2022)
Experimental Study on Horizontal
Flame Spread of Dual-Flame Sources
for Building Façade Energy
Conservation FPU Foam Under the
Effect of Lateral Wind.
Front. Energy Res. 10:887499.
doi: 10.3389/fenrg.2022.887499

The thermal safety of building façade energy conservation materials is commonly affected by the wind in the surrounding environment. In addition, multiple fire sources might be formed because of the secondary ignition of the primary fire source. In this study, the competing effect of dual flame sources and the lateral wind speed ($U_w = 0\text{m/s}, 0.5\text{m/s}, 1.0\text{m/s}, 1.5\text{m/s}, 2.0\text{m/s}$) on the typical characteristic parameters (flame morphology, mass loss rate, and heat transfer) of horizontal flame spread behavior of thermal insulation board flexible polyurethane was investigated through laboratory-scale experiments. The results showed that these parameters did not increase or decrease monotonously with the lateral wind speed. The original vertical flame front was stretched and tilted by the effect of lateral wind speed, which increased the area and thermal feedback of the preheating zone on the windward side. On the one hand, the lateral wind promoted the peak flame temperature and shortened the time to the peak temperature. On the other hand, the wind speed promoted the average flame spread velocity on the windward side and decreased the average flame spread velocity on the leeward side. The flame was blown out when the wind reached a critical speed. This could be well-explained with the mechanism of heat transfer and turbulent flow. This work can provide a reference for the fire rescue and building fire protection regulations.

Keywords: thermal insulation material, building facade, dual ignition sources, lateral wind speed, fire spread

INTRODUCTION

Building thermal insulation materials are widely used on the cladding of high-rise buildings and play a significant role in building energy conservation. Typical thermal insulation materials such as extruded polystyrene (XPS), expanded polystyrene (EPS) and flexible polyurethane (FPU) are used in building facades due to their lower density, excellent effect on thermal insulation, and economical efficiency.

However, as one of the typical high molecular polymer materials, the investigation of the fire hazard of these insulation materials takes a great count. Toxic and harmful smoke released during the combustion process boosts the fire hazard expressively. The most impressive fire cases include the fire in the Beijing TV culture center in 2009, the Shanghai “11.15” special

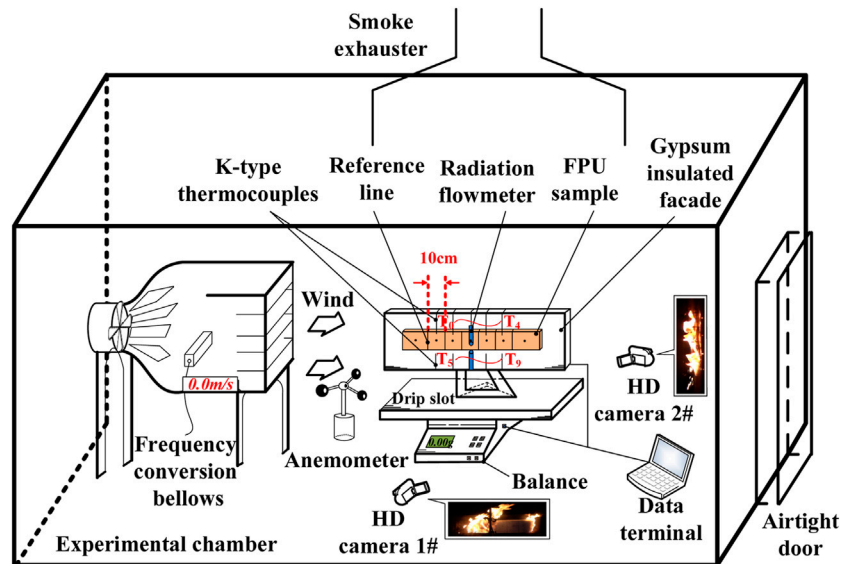


FIGURE 1 | Schematic diagram of the experimental setup for the horizontal flame spread of the FPU under the lateral wind.

major fire in 2010, and the fire accident of Grenfell Tower in London in 2017. In the fire caused by thermal insulation materials of modern high-rise building facades, the combustion behaviors are much more complex and can hardly be predicted under the influence of the natural wind. In addition, the mechanisms of burning and flame spread are quite different from those of other ordinary solid fuels because most of the polymer materials will undergo a melting and dripping process under external heating.

The molten materials that drip from the original flame area could ignite surrounding combustibles, thereby increasing the flame spread rate and expanding the fire area rapidly (Luo, 2019). Senior researchers have carried out in-depth studies on various factors affecting the flame spread process of thermal insulation materials, most of which have studied the influence of environmental pressure on the flame spread behavior (Ris et al., 1973; Wieser et al., 1997; Chow and Zou, 2009; Zhang et al., 2011). Sun and Jiang et al. (Jiang et al., 2017; Jiang et al., 2018) investigated the effects of scale (width and thickness) on acceleration propagation of horizontal and vertical flame spread over PMMA sheets. An et al. (An, 2015) have studied the influence of sample thickness, sidewalls, and atmospheric pressure on the downward flame spread over XPS. It is concluded that the thickness of the sample is positively correlated with the loss rate of combustion mass, and the average spread rate and the growth rate of the molten sample mass increase with the increase of sample thickness. Tu et al. (Tu et al., 2019) analyzed the coupling effect of environmental pressure and the angle of facade during the counter-current flame propagation of the thermal insulation material FPU. It is found that the flame tilt was determined by the asymmetric entrainment, and it is also the key factor in controlling the mechanism of thermal preheating.

In this work, the horizontal flame spread of the FPU foam board with dual-ignition sources under lateral wind speed was studied by laboratory-scale experiments. Experimental parameters such as mass loss rate, flame temperature, and radiant heat flux have been analyzed and discussed. Flame morphology and the heat and mass transfer mechanism were analyzed with image analysis and the theoretical model.

EXPERIMENTAL PROCEDURE

This work aims to investigate the lateral flame spread behavior of polyurethane under a lateral wind environment through the analysis of flame shape, near field temperature, mass loss, and flame spread during the flame spread tests. As shown in **Figure 1**, all experiments were carried out in a test chamber with constant temperature and pressure. Our experimental setup includes an adjustable system for stable lateral air supply, a horizontal flame spread system, and a data acquisition system. The lateral airflow is provided by frequency conversion bellows. A three-probe anemometer (accuracy of 0.01 m/s, range of 0–9.99 m/s) is used to monitor the lateral wind speed to ensure the accuracy and uniformity of the airflow near the specimen. In this work, five different lateral wind flow velocities ($U_w = 0\text{m/s}, 0.5\text{m/s}, 1.0\text{m/s}, 1.5\text{m/s}, 2.0\text{m/s}$) were analyzed.

The FPU sample used in the experiments was horizontally fixed on the bracket nail, and the ten micro thermocouples numbered T_0 – T_9 were also arranged in two rows on the surface of the sample to record the gas temperature profile during the flame spread. Gaps between the thermocouple and FPU surface are 2 mm approximately above the board surface. The convective heat transfer in the preheated zone and the

TABLE 1 | Properties of the FPU foam used for tests.

Average element structure	CH _{1.6} O _{0.30} N _{0.05}
Density (kg/m ³)	41.5
Specific heat (KJ/kg·K)	1.5
Dimension (long/wide/thick, cm)	80/10/2
Heat conductivity coefficient (W/m·K)	0.037
Pyrolysis temperature (K)	440
The heat of combustion (MJ/kg)	30

radiant heat flux near the flame front during the flame spread were separately recorded by two heat flow meters (STT-25-50-R/WF, Tu Xin Inc. with an accuracy of 0.01kW/m²) placed separately at the upper and lower positions of the vertical centerline of the sample.

A pan was mounted under the facade structure to collect the possible molten droplet during the burning of molten FPU. Another high-precision electronic balance (accuracy of 0.01 g, manufactured by Sartorius Co., LTD) was used to measure the mass loss of the FPU foam during the horizontal flame spread. Two HD cameras (SONY, FDR-AX100E, 50 fps) were used to monitor flame spread behaviors from the front view (1#) and side view (2#), respectively. The FPU boards used in the experiments are 80 cm long, 10 cm wide, and 2 cm thick. The detailed properties of the FPU are shown in **Table 1**.

Reference lines were drawn at an increment of 10 cm along the centerline of the FPU board. This will be convenient to record the instantaneous position of the flame front. Two propane igniters were used to ignite both sides of the sample plate at the same time. The experiment for each case was repeated thrice at least to ensure reproducibility. The smoke exhauster was only used to remove volatile matter after each experiment. All experiments were conducted at constant air temperature and relative humidity in the city of Hefei (22 ± 2.0°C, 55 ± 4%). Temperature and fuel mass data were recorded at a frequency of 1 Hz.

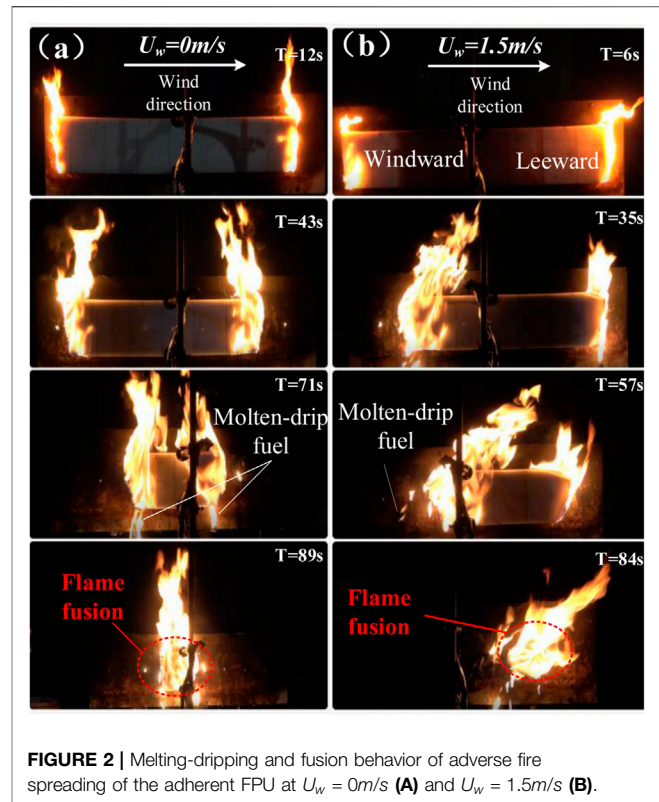
RESULTS AND DISCUSSION

Flame Morphology and Spreading Behavior

The flame spread behavior under the condition of dual ignitions includes a windward flame spread, a leeward flame spread, and the fusion of the two fire sources. The flame spread was accelerated significantly after the propane burner ignited both sides of the horizontal sample simultaneously. According to the research of Thomas (Thomas, 1963), the flame stretching effect is positively correlated with the combustion rate and wind speed. The critical condition of flame fusion is the assumption of buoyancy balance, which is derived from total airflow balance and flame thrust (Baldwin, 1968)

$$s/d = 0.14(L/d)^{0.96} \text{ with } 1 < L/d < 10, \quad (1)$$

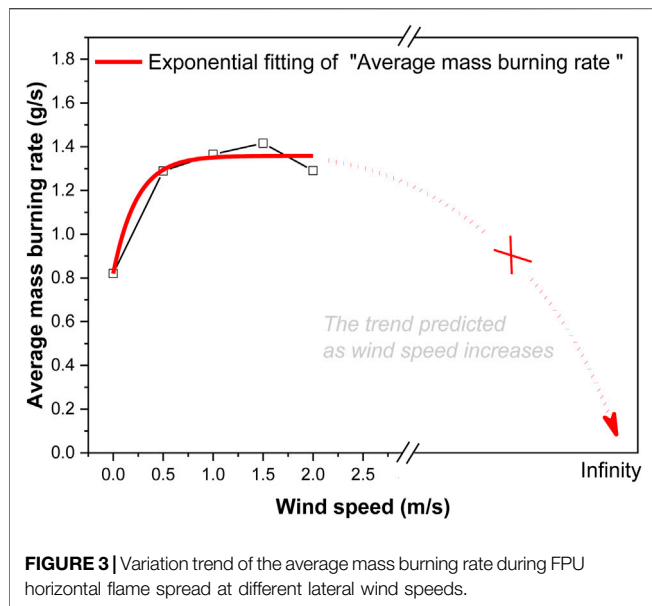
where s is the distance between fire sources, d is the size of the flame, and L is the critical flame height of the fusion flame array.

**FIGURE 2** | Melting-dripping and fusion behavior of adverse fire spreading of the adherent FPU at $U_w = 0m/s$ (A) and $U_w = 1.5m/s$ (B).

As formulated by Eq. 1, the condition for merging is independent of the number of fires.

Figures 2A,B presented the flame shape during the adherent flame spread at the wind velocities of $U_w = 0m/s$ and $U_w = 1.5m/s$, respectively. As shown in **Figure 2A**, the flame rise is almost vertically induced by the buoyancy airflow after being ignited in a windless environment. The vertical flames on both sides of the horizontal sample spread at the same speed, accompanied by random droplets. The molten fuel would detach from the flame zone and flow along the burned-out edge of the sample, which generated another new ignition source near the preheated region. Finally, two fire sources fused at the center of the horizontal sample. The pyrolysis fronts on the windward and leeward sides could be approximately regarded as one-dimensional, and there were no significant differences in the flame spread velocities on both sides of the flame ($T = 12$ s). Actually, the process of heat and mass transfer in the thickness direction of the sample is much complicated. When the pyrolysis fronts of two sides moved to the central line of the sample, the dual-flame sources met and fused, and the flame height reached its maximum at $T = 89$ s.

Compared with the windless environment, the lateral wind promoted asymmetrical air entrainment as shown in **Figure 2B**. Flame shapes were changed because of the interaction between the lateral airflow and buoyant flame. The flame on the windward side was stretched and inclined to the surface of the board ($T = 57$ s), which increased the area of the preheated zone and also promoted the heat feedback from the flame to the unburned fuel.



The upstream air entrainment can be divided into a horizontal component and vertical component, with the wind speed increased. Complex flame structures caused by wind turbulent flow and air entrainment can be observed at about 84 s. The fusion region occurred on the leeward side, which verified the tilt of the flame on the windward side. In the process of flame spread, the molten liquid drops from the flame zone with a relatively high frequency. Compared with the original flame, the inclination of the new flame formed by the fusion of the original flames on both sides is stronger ($T = 84$ s).

Mass Loss Rate and Mechanism of Heat and Mass Transfer

In actual fire accidents, dripping behaviors enhanced the thermal hazards of thermoplastic materials and made it harder for fire rescue. It is complicated to comprehensively understand the flame spread mechanism of these materials. However, the mass-loss rate can be used to reflect the heat release rate which should be directly related to the thermal feedback from the flame to the preheating zone. Therefore, the mass-loss rate is a decisive parameter to characterize the peculiarities of flame spread. Heat and mass transfer from a flame surface to the pyrolysis region play a significant role in flame spread (Jiang et al., 2014a; Jiang et al., 2014b; Jiang et al., 2017). **Figure 3** presents a comparison of mass loss data during the horizontal flame spread under different lateral wind speeds. The average mass combustion rate is obtained by linear fitting the mass loss data varying with time in the stable stage of flame spread. The results show that the mass-loss rate for the case with lateral wind speed is generally higher than that without wind obviously. With the increase in wind speed, there is a power-law relationship between the mass-loss rate and wind speed (after a series of fitting test, we found that the experimental data can be well-

fitted by the exponential function, $y = 1.36 - 0.54 \exp(-4.3x)$. This means that the loss rate is increasing all the time, and the influence of lateral wind speed on the mass-loss rate is getting weak. Under the condition without wind, the molten fuel rolls and drips intermittently under the effect of gravity. During this condition, the air convection is weak, and the oxygen required for combustion cannot be replenished in time, which induces a slow combustion rate. The lateral wind speed increases the convective heat transfer from the flame to the unburned material. The flame front on the windward side is stretched and gets closer to the sample surface, which improved the radiation heat transfer to the preheating area and thus increases the overall pyrolysis rate. Then, the mass loss under the lateral wind condition is faster than that in the windless environment.

In real fire cases, the spread phenomena such as flowing and dripping of high-temperature melt further increase the probability of flame diffusion, and it is also one of the important indicators to represent fire hazards. The drop rate of the high-temperature melt produced by the sample pyrolysis (the ratio of the droplet mass to the sample original mass) also increases with the increase of the lateral wind speed. The horizontal dynamic component must be formed by the coupling effect of gravity action of fuel and lateral wind speed, which drives the molten material away from the original flame area to form new ignition points. It indicates that ambient wind speed is positively correlated with the damage of the fire caused by the FPU.

The flame spread behavior is mainly influenced by heat and mass transfer between the flame and the pyrolysis material. The flame spread characteristics of the horizontal sample in a windless environment are affected by heat conduction from the linear pyrolysis front to the preheating zone, as shown in **Figure 4**, but this effect is very limited. The flame sources on both sides were covered and fused at the center of the horizontal sample and reached the maximum flame height immediately. It forms a thermal radiation vortex field around it with air entrainment by the flame plume, which increases the flame scale significantly. When the lateral wind speed exists ($U_w = 2.0 \text{ m/s}$), the heat transfer mechanism in the process of fire spread gradually changes to the combined action of heat conduction, radiation, and convection. The wind speed tilts the original shape of the flame plume, enhances the heat transfer from the inclined flame to the preheating area, and promotes the flow and dripping of the molten material. In addition, the flame front shows significant inclination after the fusion of the two flame resources, which is harmful in the facade fire. This should be an important factor that needs to be considered when conducting fire protection design and rescue.

The Flame Temperature and Radiant Heat Flux

According to the modified formula derived in the study by Luo, (1997), radiation correction was carried out with temperature data

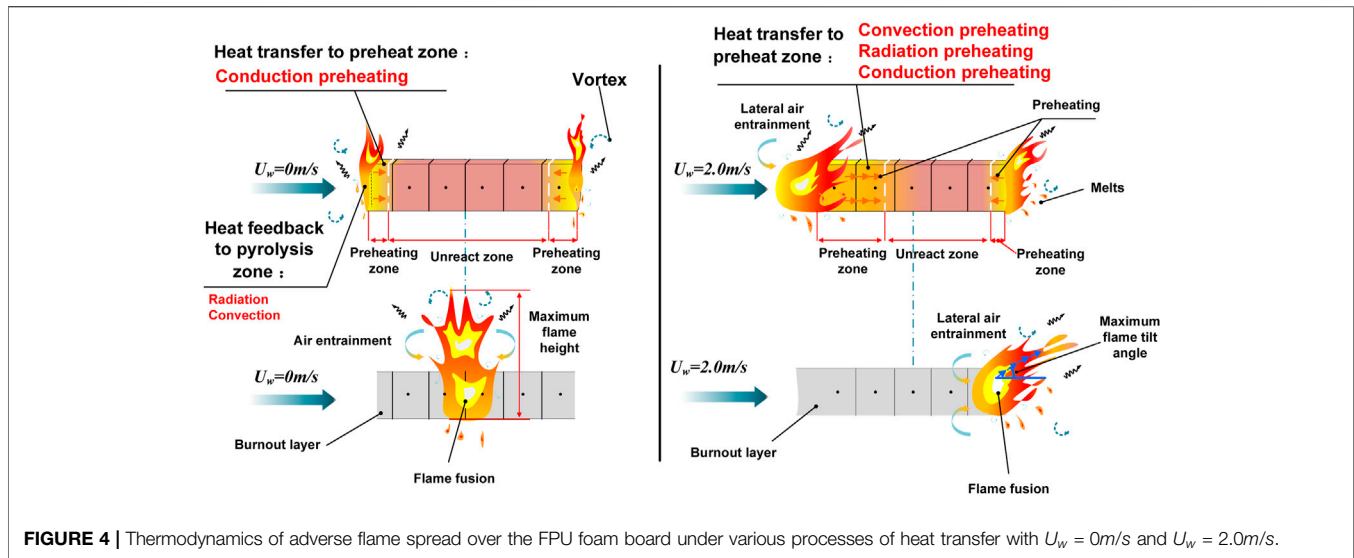


FIGURE 4 | Thermodynamics of adverse flame spread over the FPU foam board under various processes of heat transfer with $U_w = 0m/s$ and $U_w = 2.0m/s$.

$$T_g - T_{th} = \frac{\sigma \varepsilon (1 - \varepsilon_g) T_g^4}{h + 4\sigma \varepsilon T_g^3}, \quad (2)$$

where T_g is the gas temperature, T_{th} is the absolute temperature recorded by the thermocouple, h is the convective heat transfer coefficient of the thermocouple probe, σ is the Stefan–Boltzmann constant, and ε and ε_g are the emissivity values of the thermocouple and gas, respectively, and assuming that they are 0.9 and 0.1.

Figure 5 shows the temperature profile measured by two rows of thermocouples, which are 2 mm from the surface of the sample and located at the central and lateral sides of the sample board.

It can be seen from **Figure 5A** that thermocouples Group I (T_0 , T_4 , T_5 , and T_9) and Group II (T_1 , T_3 , T_6 , and T_8) heated up to the peak value of the self-spreading process almost simultaneously in a windless environment. After fusing at the place of Group III (T_2 and T_7), fire sources on both sides reached the peak temperature of 729.5 and 712.6°C in the whole spreading process at the same time and then plunged.

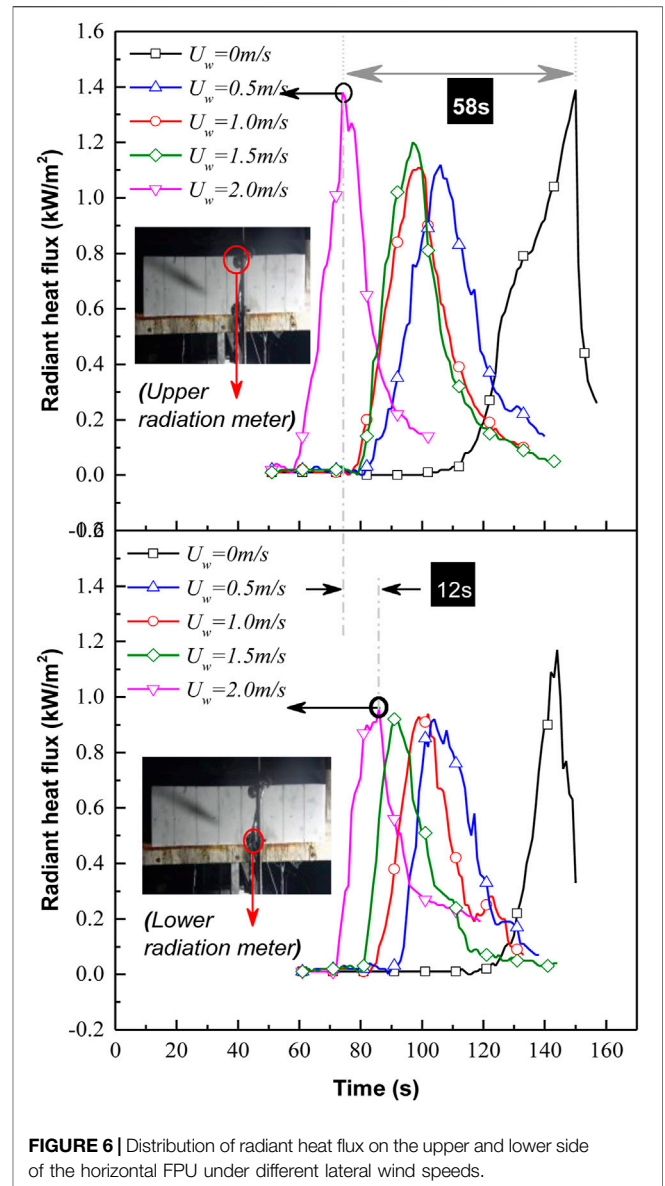
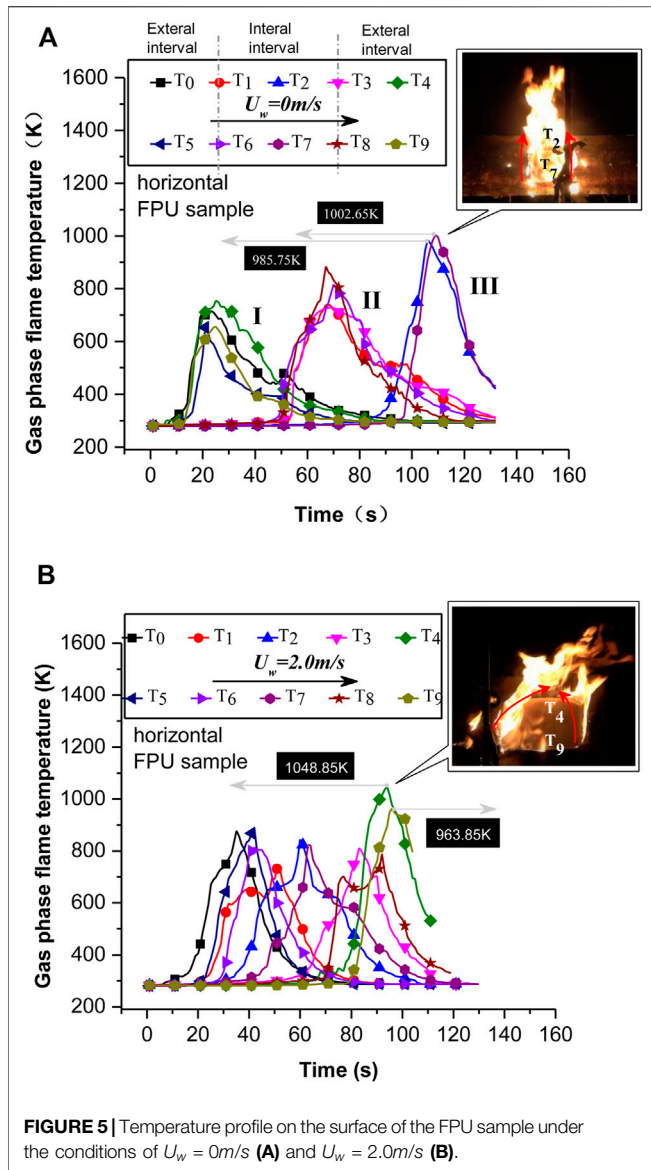
The temperatures measured by other thermocouples also decreased with the burning out of the sample. Temperature measured by the three groups shows an increasing trend in **Figure 5A**. It is shown that the flames which were in the vertical state under the buoyancy force on both sides spread uniformly along the sample surface in the absence of lateral wind. It took a significantly longer time for the two flames to migrate between the outer regions (T_0 and T_1 and T_3 and T_4) than the inner regions (T_1 and T_2 and T_2 and T_3). Most of the heat generated by sample pyrolysis has been dissipated by gas convection, which in turn heated up the outside area when the flames migrated in the outer region.

However, the distance between fire sources on two sides is close enough for thermal feedback through radiation or convection. This effect improves the flame spread rate and shortens the required time for the two flame fronts to migrate

to the inside zone. The heat accumulation rate of the dual-fire source and the heat radiation effect in the fusion stage are stronger than those in the general flame spread stage. The molten droplets caused the most significant mandatory conduction of molten liquid. The temperature of the surface increased sharply to the peak value of the whole spread process. As shown in **Figure 5B**, it is found that T_0 heated up at the fastest rate, while T_9 was the slowest. The peak temperatures of thermocouples (T_0 – T_3 and T_5 – T_8) are almost the same, and the temperature of the thermocouples on the upper side increased faster than that at the lower generally.

When $U_w = 2.0m/s$, T_4 and T_9 reach the longest heating time and the temperature tendency changed linearly approximately with peak values of 775.7 and 690.7°C, respectively. This is because the fire source on the windward side appeared to tilt under the action of lateral wind speed and fused with the flame on the leeward side at the position of T_4 , wherein heat accumulated in the preheated zone on both sides immediately ignited pyrolysis steam. Also, the temperature rises to the peak suddenly with the fire becoming stronger immediately, as shown in **Figure 5B**.

Under the coupling effect of buoyancy and lateral wind speed, the flame spread aslant along the upper side of the FPU board. This effect leads to the fastest spread speed on the upper zone of the windward side. On the contrary, the leeward flame and unburned area are in the opposite direction, which leads to less heat radiation in the preheated area and slower flame spreading speed due to the stretching effect of lateral wind. The windward side flame was inclined to a significant degree by the lateral wind and applied to the surface of the unburned area of the FPU board, and this caused an increased preheating length in unburned fuel. A couple of effects of the rapid suction flow of the flame and its thermal feedback accelerate the softening and melting of the unburned board. All these factors accelerated the whole flame migration process.



The flame spread process mainly depends on the radiation heat absorbed by the unburned area and convection heat transfer from the flame. When the external flame radiation is stronger than the heat loss of the material itself, the flame spread rate will accelerate and rise monotonously. As can be seen from **Figure 6**, the peak value of the radiant heat flux on the surface of the sample was always higher than that in the case of wind when there was no lateral wind due to the amount of radiant heat taken away by the relative ambient wind cooling effect on the upper or lower side of the board. It has taken the longest time for the horizontal spread of the flames on both sides in an environment without lateral wind, and this gives another aspect to show the least flame spread speed.

It is worth noting that as can be seen from **Figure 6**, the results for the cases of $U_w = 0\text{m/s}$, $U_w = 0.5\text{m/s}$, and $U_w = 1.5\text{m/s}$ have little difference in the heat flux of flame radiation. In addition, the flame propagation rates of the

upper and lower side were almost the same. However, the degree of flame tilt was shown more significant at $U_w = 2.0\text{m/s}$. In addition to the heat conduction in the combustion zone, the radiation effect of the inclined flame is transferred to the upper part of the board directly, which results in the flame on the upper side spreading faster than on the lower side. The peak values of radiant heat flux were 1.38 kW/m^2 and 0.96 kW/m^2 . The time difference between the upper side and lower side of the surface to reach the peak value was 12 s approximately, while the time difference between the upper side and the windless environment was about 58 s, and the upper side could be higher than the lower side generally.

It can be concluded that the lateral wind speed, on the one hand, improves the peak value of radiant heat flux on the surface of the sample and on the other hand reduces the

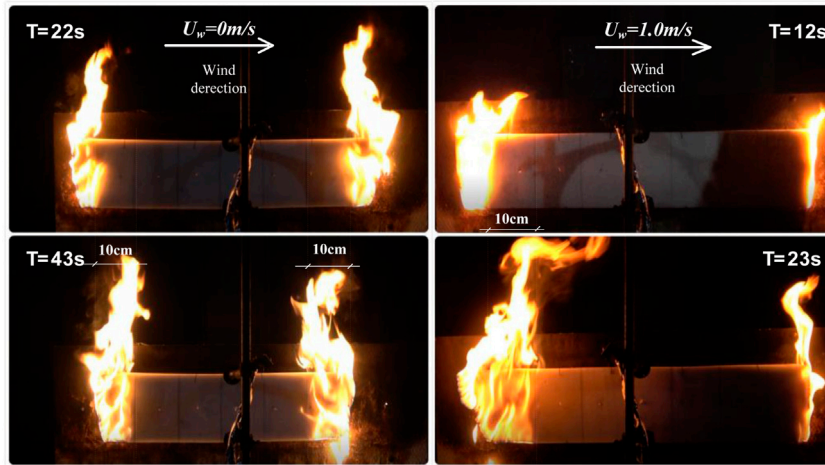


FIGURE 7 | Photographic images showing the comparison of the time required for the same intervals (10 cm) of flame migration in the different zones of FPU boards at $U_w = 0\text{m/s}$ and $U_w = 1.0\text{m/s}$.

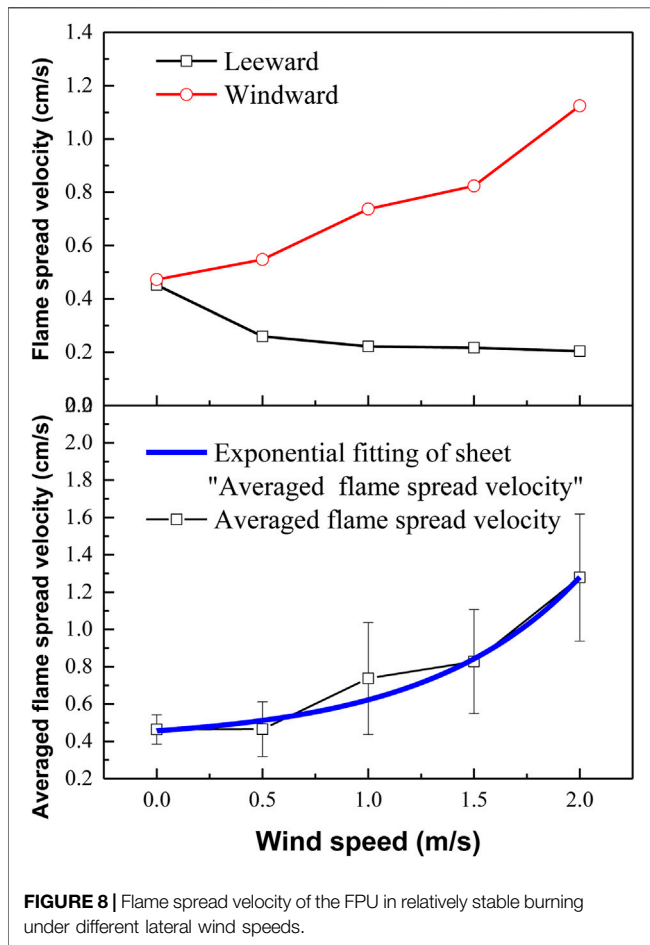


FIGURE 8 | Flame spread velocity of the FPU in relatively stable burning under different lateral wind speeds.

occurrence time of the radiant heat peak. Therefore, fire damage with the lateral wind is relatively greater than that without lateral wind.

Analysis of Flame Spread Velocity on the Leeward Side and Windward Side

The wind in the actual environment of high-rise buildings is less affected by ground friction. It is accompanied by powerful ambient wind disturbance when the fire occurs. Compared with the windless environment, the wind speed would accelerate the flame front to absorb turbulent flowing air and enhances oxygen supply in the combustion process by convection and promotes fire spread. On the other hand, the wind changes the flame shapes and orientations and increases the risk of fire in surrounding unburned areas. Many previous researchers used various physical methods such as holographic interferometry and video processing methods (Ito and Kashiwagi, 1988a; Ito and Kashiwagi, 1988b) to investigate the behaviors of pyrolysis fronts over time.

In this study, the flame spread velocity was defined as the ratio of the horizontal spread distance of the pyrolysis front to the required time in the relatively stable burning stage, as shown in Figure 7. Lines with an interval of 10 cm were drawn on the surface of the FPU board in advance. The image sequence of the flame spread process recorded by the front HD camera #1 (50 fps) was analyzed. The time required for the flame spread in each width interval was calculated to obtain the average flame spreading velocity. The measured flame spread velocities under different lateral wind speeds are shown in Figure 8.

Figure 8 shows that the relationship between the flame spread velocity on the windward side and the lateral wind speed can be fitted with a power function, and the flame spread velocity on the windward side increases with the lateral wind speed. But, the flame spread velocity on the leeward side is opposite to that of the windward side. The existence of lateral wind has changed the original state of buoyancy of the flame shape so that the windward side of the flame tilted to the unburned area, increasing the preheating area and accelerating

the melting pyrolysis rate of the fuel board. However, the leeward flame shape was stretched by the lateral wind to downwind, taking most of the heat away and reducing the spreading velocity further.

According to the general energy balance of the flame spread process, the flame spread velocity can be derived by heat transfer balance.

$$\rho_s C_s \tau V_f (T_p - T_0) = \int_{x_p}^{x_f} (\dot{q}_f'' - \dot{q}_{r,loss}'' - \dot{q}_{conv,loss}'') dx, \quad (3)$$

where C_s and ρ_s are the specific heat capacity and density of the sample sheet, respectively. T_p and T_0 are separately the pyrolysis temperature and initial temperature, respectively. \dot{q}_f'' , $\dot{q}_{r,loss}''$ and $\dot{q}_{conv,loss}''$ are the burning heat release rate, heat loss to the environment, and heat loss by mass convection, respectively. Eq. 3 is derived based on the general energy balance of the flame spread process, so this model should be applicable to thermal thin materials, including wood and polymer materials. The flame spread velocity can be expressed as

$$\begin{aligned} \rho_g C_{pg} \tau V_f (T_p - T_0) &= \frac{1}{\rho_g C_{pg} \tau (T_p - T_0)} \int_{x_p}^{x_f} (\dot{q}_f'' - \dot{q}_{r,loss}'' \\ &\quad - \dot{q}_{conv,loss}'') dx \\ &\cong \frac{(x_f - x_p)}{\rho_g C_{pg} \tau (T_p - T_0)} (\dot{q}_f'' - \dot{q}_{r,loss}'' - \dot{q}_{conv,loss}''). \end{aligned} \quad (4)$$

For the windward flame spread, x_f and x_p are separately the position's flame tip and pyrolysis. The expression $x_f - x_p$ represents the length of the flame attached to the sample surface. For the leeward flame spread, $x_f - x_p$ means the preheated length from the flame to solid fuel. The ambient wind increases the attach length $x_f - x_p$ on the windward side but decreases the preheated length $x_f - x_p$ on the leeward side.

In addition, the heat transfer by mass convection can be scaled as

$$\dot{Q}_{conv,loss} \cong U_\infty C_{pg} \rho_g (T_f - T_0), \quad (5)$$

where U_∞ is the wind velocity. C_{pg} and ρ_g are the specific heat capacity and density of the gas, respectively. T_f and T_0 are separately the flame temperature and initial airflow temperature, respectively.

The heat transfer by mass convection of the airflow at the windward side can still transfer to the sample surface away from the flame front position; thus, the heat transfer by mass convection plays a positive role in flame spread velocity at the windward side. However, heat transfer by the mass convection cannot transfer to the material at the leeward side because the convective heat is transferred to the opposite direction of flame spread. According to Eq. 5, heat transfer by mass convection increases with wind velocity. Consequently, the flame spread rate at the leeward side may decrease with the wind speed. This work explained the flame spread behavior with some fundamental theory of heat and mass transfer, which has been widely used

in previous literature to verify their reliability. The heat conduction of FPU foam and the heat convection of flame depend on the detailed information of material temperature field and gas-phase temperature field, which will be analyzed in our subsequent work.

The ambient wind made the fluctuating developed fire plume disturbed and enhanced the air convection, and the combustion of the board in the preheating zone has been promoted. Thus, the burning rate of the board is faster than that in windless condition. As shown in Figure 8, by increasing the lateral wind speed, flame spread velocity would increase, which might be caused by the increasing heat released by material melting and gasification. Moreover, the heat transfer and solid phase heat conduction would also increase the flame spread rate. The intensity of flame oscillation would be enhanced, and the radiation heat from the oscillating flame increased in the preheating zone so that the combustion rate of the sample itself tended to increase.

With the increase in wind speed, the proportion of heat transfer mechanisms in the combustion process of the board has been changed. At this time, thermal feedback enhancement played a dominant role with air entrainment being limited with the flame oscillating violently and significantly tilting angle. The flame front of the initial phase under the effect of buoyancy morphogenesis significantly tilt vertically, flames elongated, and sticking with the board surface which increases the preheating zone area and heat feedback. The flame front also had an obvious power-law fitting with time, which meant that the flame spread rate accelerated all the time. The preheating zone was subjected to the thermal radiation of the oscillating flame to accelerate the accumulation of its heat, and the pyrolysis rate increased greatly, which accelerated the flame migration process.

CONCLUSION

In this work, a series of control experiments were conducted to investigate the effects of external wind velocity on the flame spread of the FPU board with dual-ignition sources. The flame morphology, mass loss rate, flame temperature profile, and flame velocity were analyzed based on the heat transfer mechanism and fire dynamics. Major conclusions are summarized as follows:

- 1) The lateral wind changed the flame shape in the vertical direction, and the flame was stretched and inclined to the surface of the board, which increased the area of the preheating zone and heat transfer from the flame to the unburned solid. Heat accumulated faster in the preheating zone.
- 2) The mass-loss rate gradually increased with the lateral wind velocity and then reaches to steady state with the increase of wind speed. The flame was blown out when the wind reached a critical speed. This could be well-explained with the mechanism of heat transfer and turbulent flow.
- 3) The lateral wind enhanced the peaks of heat radiation and the temperature and reduced the time reach to the peak value compared with the case without lateral wind. The peak

temperature in the middle of the board is higher than that on the two sides.

- 4) The flame spread velocities on the windward side and the leeward side were positively and negatively correlated with the lateral wind velocity, respectively. Based on the stretching effect of lateral wind speed, it can be concluded that the heat transfer from the tilted flame to the unburned solid dominated the horizontal burning.

DATA AVAILABILITY STATEMENT

The original contributions presented in the study are included in the article/Supplementary Material; further inquiries can be directed to the corresponding author.

REFERENCES

- An, W. G. (2015). Downward Flame Spread Over Extruded Polystyrene Effects of Sample Thickness, Pressure, and Sidewalls. *J. Therm. Anal. Calorim.* 119, 1091–1103. doi:10.1007/s10973-014-4186-4
- Baldwin, R. (1968). Flame Merging in Multiple Fires. *Combust. Flame* 12, 318–324. doi:10.1016/0010-2180(68)90036-9
- Chow, W. K., and Zou, G. W. (2009). Numerical Simulation of Pressure Changes in Closed Chamber Fires. *Build. Environ.* 44, 1261–1275. doi:10.1016/j.buildenv.2008.09.016
- Ito, A., and Kashiwagi, T. (1988). Temperature Measurements in PMMA during Downward Flame Spread in air Using Holographic Interferometry. *Symposium Int. Combust.* 21 (1), 65–74. doi:10.1016/s0082-0784(88)80232-7
- Ito, A., and Kashiwagi, T. (1988). Characterization of Flame Spread over PMMA Using Holographic Interferometry Sample Orientation Effects. *Combust. Flame* 71, 189–204. doi:10.1016/0010-2180(88)90007-7
- Jiang, L., He, J.-J., and Sun, J.-H. (2018). Sample Width and Thickness Effects on Upward Flame Spread Over PMMA Surface. *J. Hazard. Mat.* 342, 114–120. doi:10.1016/j.jhazmat.2017.08.022
- Jiang, L., Miller, C. H., Gollner, M. J., and Sun, J.-H. (2017). Sample Width and Thickness Effects on Horizontal Flame Spread Over a Thin PMMA Surface. *Proc. Combust. Inst.* 36, 2987–2994. doi:10.1016/j.proci.2016.06.157
- Jiang, L., Xiao, H., An, W., Zhou, Y., and Sun, J. (2014). Correlation Study between Flammability and the Width of Organic Thermal Insulation Materials for Building Exterior Walls. *Energy Build.* 82, 243–249. doi:10.1016/j.enbuild.2014.06.013
- Jiang, L., Xiao, H., Zhou, Y., An, W., Yan, W., He, J., et al. (2014). Theoretical and Experimental Study of Width Effects on Horizontal Flame Spread over Extruded and Expanded Polystyrene Foam Surfaces. *J. Fire Sci.* 32 (3), 193–209. doi:10.1177/0734904113505677
- Luo, M. C. (1997). Effects of Radiation on Temperature Measurement in a Fire Environment. *J. Fire Sci.* 15 (6), 443–461. doi:10.1177/073490419701500602

AUTHOR CONTRIBUTIONS

WZ is mainly responsible for experimental data collation, literature research, manuscript writing, and submission. JW is mainly responsible for the design of the experimental scheme, experimental execution, and data processing.

FUNDING

This work was supported by the Anhui Provincial Natural Science Foundation of China (Grant No. 1908085QE250).

ACKNOWLEDGMENTS

The authors gratefully acknowledge all these supports.

Luo, S. F. (2019). *Dynamic Characteristic of Melting Layer in Flame Front during Downward Flame Spread of XPS Foam*. Shenzhen, China: University of Technology and Science of China.

Ris, J. D., Murty Kanury, A., and Yuen, M. C. (1973). Pressure Modeling of Fires. *Symposium Int. Combust.* 14, 1033–1044. doi:10.1016/s0082-0784(73)80093-1

Thomas, P. H. (1963). The Size of Flames from Natural Fires. *Proc. Combust. Inst.* 9 (1), 844–859. doi:10.1016/b978-1-4832-2759-7.50093-5

Tu, R., Ma, X., Zeng, Y., Zhou, X., He, L., Fang, T., et al. (2019). Coupling Effects of Pressure and Inclination on Downward Flame Spread Over Flexible Polyurethane Foam Board. *Build. Environ.* 164, 106339. doi:10.1016/j.buildenv.2019.106339

Wieser, D., Jauch, P., and Willi, U. (1997). The Influence of High Altitude on Fire Detector Test Fires. *Fire Saf. J.* 29, 195–204. doi:10.1016/s0379-7112(96)00042-2

Zhang, Y., Huang, X., Wang, Q., Ji, J., Sun, J., and Yin, Y. (2011). Experimental Study on the Characteristics of Horizontal Flame Spread Over XPS Surface on Plateau. *J. Hazard. Mater.* 189, 34–39. doi:10.1016/j.jhazmat.2011.01.101

Conflict of Interest: The authors declare that the research was conducted in the absence of any commercial or financial relationships that could be construed as a potential conflict of interest.

Publisher's Note: All claims expressed in this article are solely those of the authors and do not necessarily represent those of their affiliated organizations, or those of the publisher, the editors, and the reviewers. Any product that may be evaluated in this article, or claim that may be made by its manufacturer, is not guaranteed or endorsed by the publisher.

Copyright © 2022 Zhang and Wang. This is an open-access article distributed under the terms of the Creative Commons Attribution License (CC BY). The use, distribution or reproduction in other forums is permitted, provided the original author(s) and the copyright owner(s) are credited and that the original publication in this journal is cited, in accordance with accepted academic practice. No use, distribution or reproduction is permitted which does not comply with these terms.